Available online at www.sciencedirect.com
SCIENCE DIRECT®
Biochemical and Biophysical Research Communications 300 (2003) 223–229
BBRC
www.elsevier.com/locate/ybbrc

Structure determination and conformational change induced by tyrosine phosphorylation of the N-terminal domain of the α-chain of pig gastric H^+/K^+-ATPase

Naoki Fujitani,[a] Motoi Kanagawa,[b] Tomoyasu Aizawa,[a] Tadayasu Ohkubo,[c] Shunji Kaya,[b] Makoto Demura,[a] Keiichi Kawano,[d,*] Shin-ichiro Nishimura,[a] Kazuya Taniguchi,[b] and Katsutoshi Nitta[a]

[a] *Division of Biological Sciences, Graduate School of Science, Hokkaido University, Sapporo 060-0810, Japan*
[b] *Division of Chemistry, Graduate School of Science, Hokkaido University, Sapporo 060-0810, Japan*
[c] *Biophysical Chemistry, Graduate School of Pharmaceutical Sciences, Osaka University, Osaka 565-0871, Japan*
[d] *Faculty of Pharmaceutical Sciences, Toyama Medical and Pharmaceutical University, Toyama 930-0194, Japan*

Received 12 November 2002

Abstract

It has been well established that phosphorylation is an important reaction for the regulation of protein functions. In the N-terminal domain of the α-chain of pig gastric H^+/K^+-ATPase, reversible sequential phosphorylation occurs at Tyr 10 and Tyr 7. In this study, we determined the structure of the peptide involving the residues from Gly 2 to Gly 34 of pig gastric H^+/K^+-ATPase and investigated the tyrosine phosphorylation-induced conformational change using CD and NMR experiments. The solution structure showed that the N-terminal fragment has a helical conformation, and the peptide adopted two α-helices in 50% trifluoroethanol (TFE) solvent, suggesting that the peptide has a high helical propensity under hydrophobic conditions. Furthermore, the CD and NMR data suggested that the structure of the N-terminal fragment becomes more disordered as a result of phosphorylation of Tyr 10. This conformational change induced by the phosphorylation of Tyr 10 might be an advantageous reaction for sequential phosphorylation and may be important for regulating the function of H^+/K^+-ATPase.

Keywords: H^+/K^+-ATPase; Tyrosine phosphorylation; NMR; CD; Helical conformation

In general, reversible phosphorylation is one of the most common mechanisms for the regulation of protein functions. Because phosphorylation induces structural changes that involve the secondary and tertiary structures, structural analyses of the phosphorylated and unphosphorylated forms are important for investigating the structure–function relationship. Thus, for example, Laczko et al. [1] observed a conformational change of Tyr-based immunoreceptor activation motifs of the T cell receptor/CD3 ζ-chain using circular dichroism (CD) and Fourier-transform infrared (FTIR) spectroscopy. It has also been reported that the N-terminal domain of the P protein of the Chandipura virus shows a conformational change induced by phosphorylation [2]. This conformational alteration induces homodimerization in order to change the sites of the digestion of various proteases [3]. Recently, the fragment structure of the myosin phosphatase inhibitor protein CPI-17 has been determined by nuclear magnetic resonance (NMR) spectroscopy, and the results clearly show phosphorylation-induced conformational changes [4].

Gastric H^+/K^+-ATPase (gastric proton pump) is abundant in parietal cells, which secretes H^+ into the gastric lumen and electro-neutral exchange for extracellular K^+ [5]. The H^+/K^+-ATPase is categorized as a member of the family of P2-type ATPases, which includes the Na^+/K^+-ATPases and the Ca^{2+}-ATPases, because of the formation of phosphoaspartate intermediate during ATP hydrolysis. P2-type ATPases are

* Corresponding author. Fax: +81-76-434-5061.
E-mail address: kawano@ms.toyama-mpu.ac.jp (K. Kawano).

0006-291X/02/$ - see front matter © 2002 Elsevier Science (USA). All rights reserved.
PII: S0006-291X(02)02794-8

composed of a catalytic α-chain and a glycosylated β-chain. It has been shown that the α-chain of pig gastric H^+/K^+-ATPase preparations containing kinases and phosphatases displayed reversible phosphorylation of Tyr 7, Tyr 10 [6], and Ser 27 [7]. With regard to tyrosine phosphorylation, the phosphorylation of Tyr 10 precedes the phosphorylation of Tyr 7 [6]. Recently, it has been revealed that the reversible tyrosine phosphorylation of the α-chain is carried out by c-Src and a membrane-binding tyrosine phosphatase, and that the reversible serine phosphorylation is carried out by a Ca^{2+}-dependent protein kinase C and a protein phosphatase type-1 [8]. The in vivo Tyr-phosphorylation of the α-chain has also been shown using a cellular tyrosine phosphatase inhibitor [9]. According to these studies on H^+/K^+-ATPase, the reversible tyrosine phosphorylation of the H^+/K^+-ATPase α-chain might play some physiological role in the gastric parietal cells.

Although there are various reports concerning the protein phosphorylation of the N-terminal domain of P2-type ATPase [10–15], there have been few structural analyses of the N-terminal phosphorylation domain. This is the first conformational study of the N-terminal domain of P2-type ATPases. Here, we determined the three-dimensional structures of the peptide comprising the N-terminal 33 residues of the α-chain of pig gastric H^+/K^+-ATPase in both the presence and absence of trifluoroethanol (TFE), and showed the conformational change induced by phosphorylation at Tyr 10.

Materials and methods

Peptide preparation. Non-phospho- and phospho-peptides containing the 33 N-terminal amino acids of pig gastric H^+/K^+-ATPase (Gly^2–Gly^{34}) based on the sequence of the pig H^+/K^+-ATPase α-chain, i.e., $N33^{np}$ (GKAENYELYQVELGPGPSGDMAAKMSKKK AGRG; 2–34), and $N33^{pY10}$ that had been phosphorylated at Tyr 10 of $N33^{np}$, were synthesized by Sawady Technology (Tokyo, Japan).

Circular dichroism. All measurements were performed on a Jasco J-725 spectropolarimeter (Jasco, Japan). Spectra were recorded at 25 °C and at peptide concentrations of 0.02–2.0 mM using a quartz cell with a path length of 0.2–10 mm. All of the spectra were baseline-corrected by subtracting 10 mM phosphate buffer spectra. The effect of peptide concentration on the far-UV CD spectra in TFE was determined by acquiring three kinds of spectra at peptide concentrations of 0.02, 0.2, and 2.0 mM. The recorded spectra showed no dependence on the peptide concentrations. The helical content (f_H) was estimated from the ellipticity value at 222 nm ($[\theta]_{222}$) as described by Chen et al. [16] according to the following formula: $f_H = -([\theta]_{222} + 2340)/30,300$.

NMR spectroscopy and structure calculations. The samples used for NMR experiments contained 300 μl of 2 mM synthetic peptide in 90% H_2O/10% D_2O, 99.9% D_2O, and 50% H_2O/50% 2,2,2-trifluoroethanol-d_2 (TFE-d_2) at pH 4.0 with a 10 mM phosphate buffer. Furthermore, TFE-d_3 was also used for the experiments regarding hydrogen–deuterium exchange. All NMR experiments were performed on Bruker DRX 600, Bruker DMX 500, JEOL alpha 600, and Varian Unity-plus 750 spectrometers with a sample temperature of 25 °C. TOCSY spectra with a MLEV-17 sequence [17,18] were collected with spin-lock times of 45 and 100 ms, and NOESY spectra [19] were obtained with mixing times of 150, 250, 300, and 500 ms. The proton chemical shifts were referenced to external sodium 3-(trimethylsilyl) propionate-2,2,3,3-d_4 (TSP). All two-dimensional spectra were processed using NMRPipe software [20]. Time domain data in both dimensions were multiplied by a 90° phase shift sine bell window function prior to Fourier transformation. Signal assignments were achieved using XEASY software [21].

Structure calculations to determine the three-dimensional structure were run on the program X-PLOR 3.851 [22]. The calculations were initiated from generating structures having random torsion angles, and subsequently, the substructure distance geometry calculation was carried out with the only distance restraints being those of backbone atoms. Subsequently, subembedded structures were regularized with all distance restraints. Finally, regularized structures were refined with the initial temperature set at 2000 K and with 15,000 cooling steps. A total of 114 and 271 distance restraints were used to calculate the family of structures in water and TFE solution, respectively. Distance restraints for the calculations were estimated from the cross-peak intensities in NOESY spectra with a mixing time of 150 ms, and the estimated restraints were classified as strong, medium or weak and were assigned upper limits of 2.7, 3.5, and 5.0 Å, respectively; 1.6 Å was assigned as the lower limit for all restraints. The obtained structures were checked using PROCHECK [23] and MOLMOL software [24].

Results and discussion

Structure determination of the N-terminal fragment of the α-chain of pig gastric H^+/K^+-ATPase

In order to reveal the conformation of the N-terminal region of the α-chain of pig gastric H^+/K^+-ATPase, two peptides, $N33^{np}$ and $N33^{pY10}$, were synthesized. The former contained the N-terminal region of pig gastric H^+/K^+-ATPase (Gly 2–Gly 34) without the phosphate group at Tyr 10, and the latter contained the same region but with the phosphate group at Tyr 10. Because the phosphorylation of Tyr 10 occurs before the phosphorylation of Tyr 7 via an endogenous Tyr-kinase [6], we designed a phosphopeptide fully phosphorylated at Tyr 10.

Primarily, we determined the structure of $N33^{np}$ in the presence or absence of TFE using the NMR experiments and distance geometry/simulated annealing calculations. The far-UV CD spectra were recorded for $N33^{np}$ in the presence of different TFE concentrations (0–70%, v/v) (Fig. 1). TFE is well known as a helicogenic solvent that produces non-polar environments. The CD spectra with sample concentrations of 2.0, 0.2, and 0.02 mM were observed to have the same pattern and ellipticity as each other; therefore the obtained CD spectra did not depend on the peptide concentration. The CD data suggested that the α-helical content was increased with increasing TFE concentration, thus suggesting that $N33^{np}$ might have an inherent helical propensity in a more hydrophobic system such as TFE solution. Although the α-helical content of $N33^{np}$ was estimated to be 3.8% in water by the method of Chen et al. [16], that estimate was enhanced to 49% (approxi-

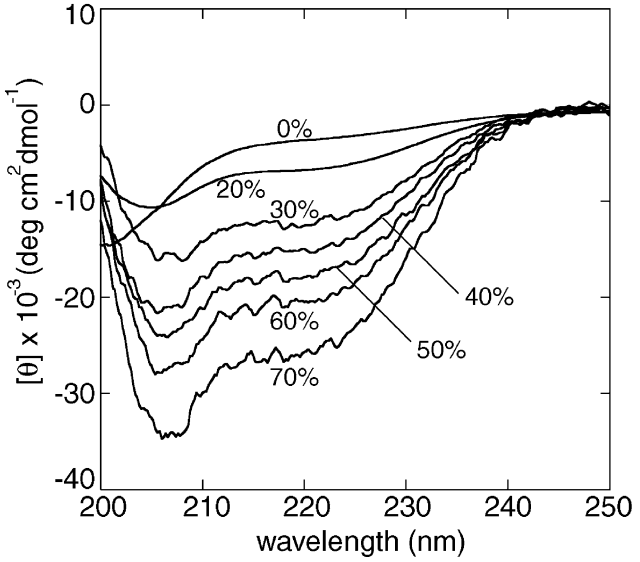

Fig. 1. Far-UV CD spectra of $N33^{np}$ in various TFE concentrations at 25 °C. The numbers near the curves indicate the percentage of TFE in the aqueous buffer (v/v).

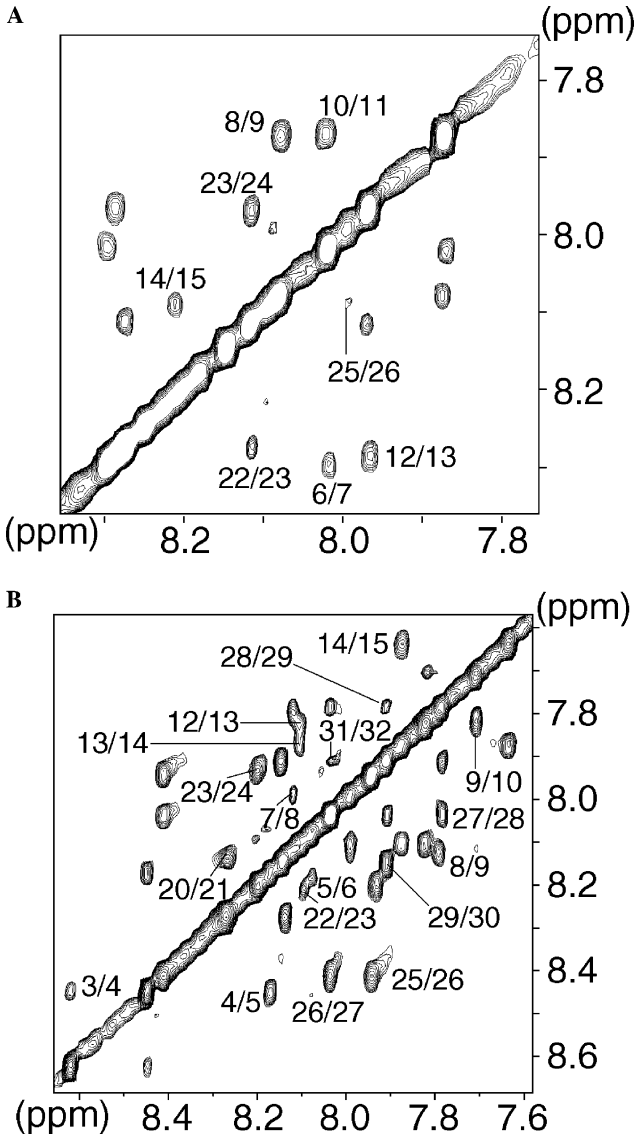

Fig. 2. Six hundred megahertz two-dimensional NOESY spectra of $N33^{np}$ in water (A) and in 50% (v/v) TFE (B) recorded at 25 °C.

mately 16 residues) in the case of 50% (v/v) TFE solution.

The NMR spectra of $N33^{np}$ under aqueous conditions supported the results of the CD experiments. Some of the NMR signals overlapped, which indicated that $N33^{np}$ might be rich in random conformations in water solution; therefore, complete assignments were difficult to achieve. Though the NOEs derived from Lys 25 and Ala 31 were unfortunately not found in NOESY spectra, all of the other signals could be assigned. Eight of the sequential NH–NH NOEs were observed with strong intensity under aqueous conditions (Fig. 2A). This observation suggested that the $N33^{np}$ has the propensity to adopt a helical structure [25]. Furthermore, the medium-range NOEs were also observed in the region from Leu 9 to Leu 14, specifically between αH of Leu 9 and βH of Val 12, between αH of Leu 9 and γH of Val 12, between βH and δH of Tyr 10 and γH of Val 12, and between γH of Val 12 and αH of Leu 14. However, no residues with a slowly exchanging rate of amide protons were identified by the hydrogen–deuterium exchange experiment, which suggest that the regular stable secondary structures with hydrogen bonds were not contained in $N33^{np}$. The structures obtained by the calculations with distance restraints derived from NMR experiments are shown in Fig. 3. Though most of the region was highly disordered, the residues between Leu 9 and Leu 14 could be well defined within 0.38 ± 0.14 Å of the backbone RMSD value. The medium-range NOEs in the region from Leu 9 to Leu 14 might derive these local converged structures with the helical conformation. Particularly, Tyr 10 and Gln 11 take a typical conformation of the helix structure with dihedral angles ϕ of $-78.1 \pm 7.5°$ and $-90.5 \pm 1.8°$, and ψ of $0.6 \pm 5.9°$ and $37.0 \pm 4.2°$, respectively. Although the structure of $N33^{np}$ in water contains a local converged conformation in the region between Leu 9 and Leu 14 based on the NMR experiments and structure calculations, the obtained structures shown in Fig. 3 might be in dynamic equilibrium with unfolded states. Therefore, the α-helix content of 3.8% obtained from the CD spectrum is a reasonable value and suggests this equilibrium state.

A crystal structure with a 2.6 Å resolution revealed that the rabbit Ca^{2+}-ATPase possesses 10 transmembrane helices [26], a feature that is believed to be common to this family of proteins, and the structure is described in the structural studies on H^+/K^+-ATPase [27]. According to the structure of the N-terminal domain of the α-chain of the Ca^{2+}-ATPase, the first helix,

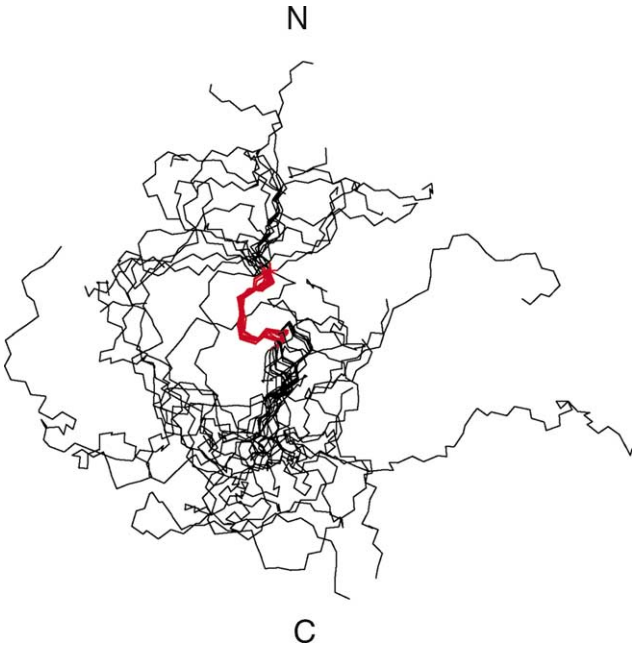

Fig. 3. Solution structures of $N33^{np}$ in aqueous solution. The backbone rendering of 15 converged structures of $N33^{np}$, superimposed on the region from Glu 8 to Val 11, is indicated in red. This figure was generated by MOLMOL [24].

including Thr 9–Phe 16, is close to the other domain that is predominantly occupied by a β-sheet, and this helix may be able to interact with the corresponding domain by hydrophobic interaction. We therefore also determined the structure of $N33^{np}$ in 50% (v/v) TFE. The assignments of NOESY spectra of the 50% (v/v) TFE sample were achieved completely, and they showed the characteristic NOEs for the helical structure in the regions including the residues Glu 5–Glu 13 and Ala 24–Lys 29. Sequential NH–NH NOEs were also increased relative to those of the $N33^{np}$ without TFE (Fig. 2B). The hydrogen–deuterium exchanging experiment also revealed that the residues of Leu 9–Glu 13 and Lys 28–Lys 29 have slowly exchanging amide protons, suggesting that these residues could form the hydrogen bonds. Obtained structures of $N33^{np}$ under the 50% TFE condition clearly adopted two α-helices comprised of the residues Glu 5–Glu 13 and Ala 24–Lys 29 (Fig. 4). The helical content of the obtained structures was 45.5% (15 residues), which strongly supported the result of CD experiments. The average backbone RMSD values of regions Glu 5–Glu 13 and Ala 24–Lys 29 were 0.28 ± 0.06 and 0.33 ± 0.08 Å, respectively, when the corresponding regions were superimposed. The residues from 15 to 18, Gly–Pro–Gly–Pro, apparently serve as a flexible linker, and no long-range NOEs were observed between the two helices, suggesting that these helices exist independently without interacting with one another. Here we showed that the N-terminal fragment of gastric H^+/K^+-ATPase adopts the stable helices under the hydrophobic condition like as TFE solution. In the case of the N-terminal region of Ca^{2+}-ATPase, a kind of P2-type ATPase, also has the bihelical structure, and could be stabilized by domain-domain interaction based on the structural analysis [26]. Furthermore it has been reported that the N-terminal domain of gastric H^+/K^+-ATPase interacts with another protein, namely the spectrin-binding domain of ankyrin III [28]. The obtained structure in this study suggests that, prior to the phosphorylation of tyrosines, the N-terminal domain of gastric H^+/K^+-ATPase might be also stabilized by the hydrophobic environment produced by intra- or intermolecular interactions.

The coordinates for the 15 lowest-energy structures of $N33^{np}$ with and without TFE have been deposited at the protein data bank (PDB) with the codes 1IWC and 1IWF, respectively.

Conformational change induced by tyrosine phosphorylation

In order to analyze the conformational change of the N-terminal domain of the α-chain of pig gastric H^+/K^+-ATPase, we also measured the CD and NMR spectra of $N33^{pY10}$. These CD and NMR experiments clearly displayed evidence of the conformational change of the N-terminal fragment of the α-chain of pig gastric H^+/K^+-ATPase (Fig. 5). The CD spectra of $N33^{pY10}$ confirmed that the spectra did not depend on the sample concentrations such as $N33^{np}$, which indicated that $N33^{pY10}$ does not aggregate non-specifically. Fig. 5A represents a comparison of the CD spectra of $N33^{pY10}$ and $N33^{np}$ in the presence or absence of 20% (v/v) TFE. The CD spectra of $N33^{pY10}$ were characteristic for random coil conformations; no significant content of α-helix or β-sheet could be detected. Peptides with a pronounced helical propensity often show the characteristic spectrum for the helical structure in a CD spectrum at much lower TFE concentrations [29]. In the case of $N33^{pY10}$, however, the spectra of $N33^{pY10}$ were not much affected by the change of solvent, showing only a very small change in ellipticity upon the addition of 20% (v/v) TFE. Therefore $N33^{pY10}$ does not have a high propensity to form the helical conformation.

The NMR experiments on the phosphorylated peptide $N33^{pY10}$ also supported the conformational change effected by tyrosine phosphorylation at Tyr 10. In the comparisons of NOESY spectra of $N33^{np}$ and $N33^{pY10}$, the spectrum of $N33^{pY10}$ showed poorer signal dispersion than that of $N33^{np}$ under aqueous conditions (Figs. 5B and C), so only a few NOEs of $N33^{pY10}$ could be assigned due to severe signal overlap. Furthermore, only three signals could be observed in the NH–NH region of NOESY spectra though eight NOEs were observed in the case of $N33^{np}$ in the corresponding region (Figs. 2A and 5D). These comparisons of the NMR spectra of

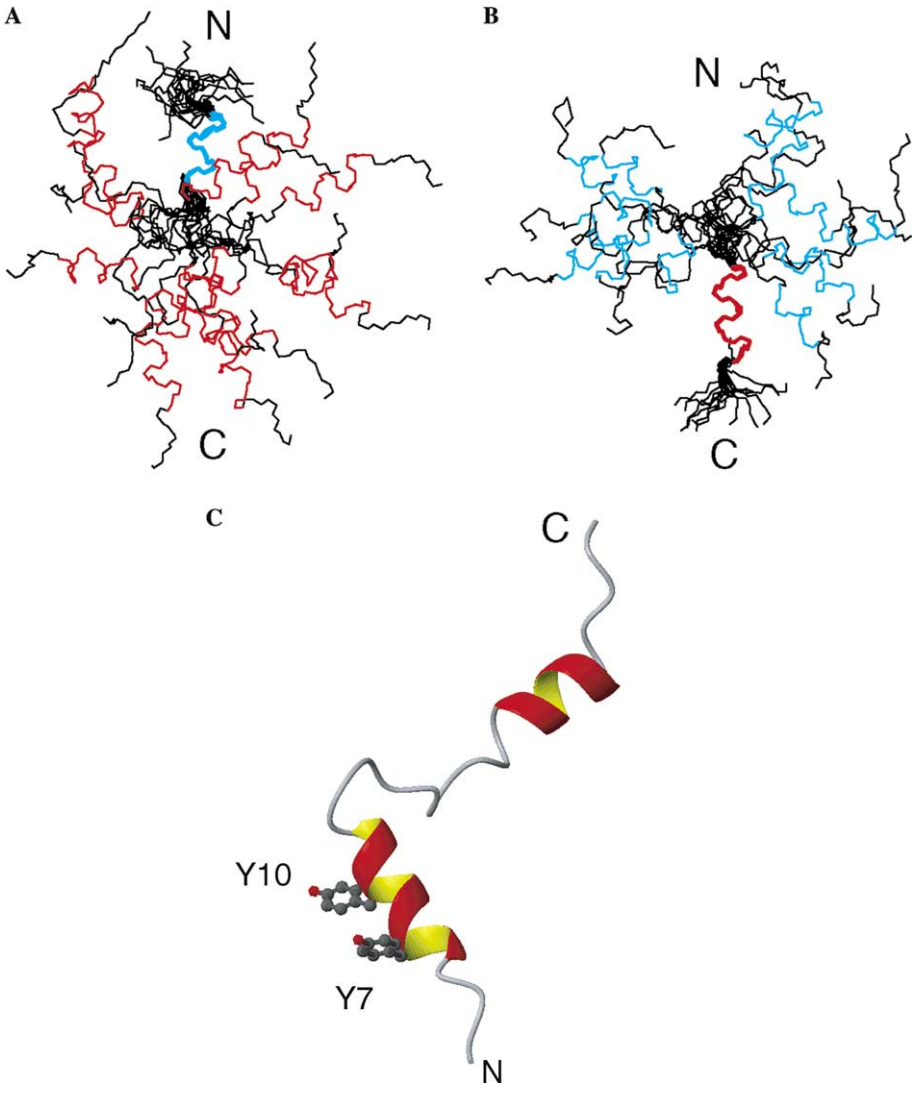

Fig. 4. Solution structures of $N33^{np}$ in the presence of 50% (v/v) TFE. (A and B) Backbone renderings of the 15 converged structures of $N33^{np}$ are superimposed on the region of Glu 5–Glu 13 (blue) and Ala 24–Lys 29 (red), respectively. (C) The ribbon diagram of the lowest energy structure with the sites of phosphorylation, Tyr 7 and Tyr 10, represented by ball-stick models. All figures were generated by MOLMOL [24].

$N33^{np}$ and $N33^{pY10}$ clearly revealed that the conformational change was induced by the tyrosine phosphorylation at Tyr 10, and these data coincided with the results of the CD experiments.

The results of the determination of the structure of $N33^{np}$ revealed that the average distances between the hydroxyl groups of the sequentially phosphorylatable tyrosines, Tyr 10 and Tyr 7, were 11.49 ± 0.65 and 11.52 ± 2.51 Å in the presence and absence of TFE, respectively. This structural information indicates that the adoption of the helical structure results in a close distance between the two phosphorylatable tyrosines than the case of extended structure (average distance is 14.98 ± 2.21 Å for 50 random structures generated by X-PLOR). However, closing the distance between the phosphorylatable tyrosines by adopting a helical structure might be less favorable for the sequential phosphorylations of Tyr 10 and Tyr 7 due to the electrostatic repulsion. Therefore, the conformational change resulting from the first phosphorylation at Tyr 10 may be an advantageous action for the sequential phosphorylations of Tyr 10 and Tyr 7. Due to the collapse of the helical conformation, Tyr 7 could be phosphorylated easily as a result of the exclusion of the electrostatic repulsion. It has been reported that tyrosine phosphorylation occurs in rat Na^+/K^+-ATPase [30]. Though the conformational change of Na^+/K^+-ATPase induced by the phosphorylation has not yet been clarified, we consider such a change likely to occur. This conformational change may also act as an important regulator to activate P2-type ATPase as an ionic pump.

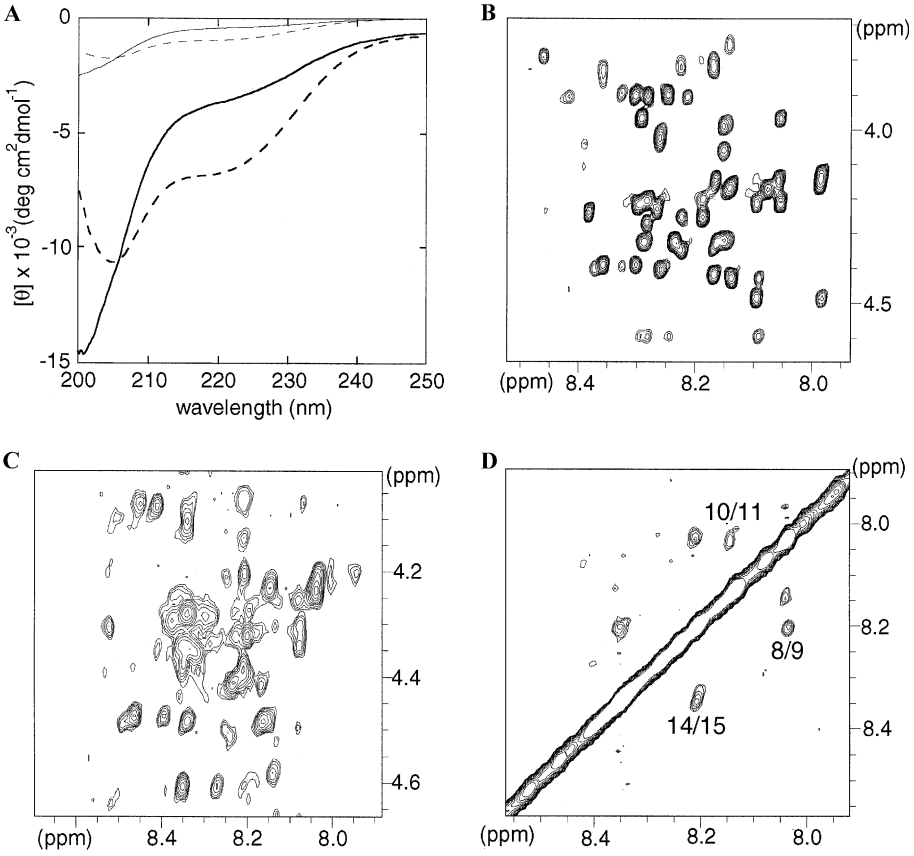

Fig. 5. CD spectra (A) and NOESY spectra (B–D) of $N33^{np}$ and $N33^{pY10}$. The thick and thin lines in the CD spectra (A) represent the spectra of $N33^{np}$ and $N33^{pY10}$, respectively, and the broken and continuous lines represent the spectra with and without 20% (v/v) TFE, respectively. NOESY spectra shown in (B) and (C) are fingerprint (αH-NH) regions of $N33^{np}$ and $N33^{pY10}$, respectively, recorded in aqueous solution. NOESY spectrum shown in (D) represents NH–NH region of $N33^{pY10}$ with assignment labels.

Acknowledgments

We thank Professor Shin-ichi Tate of Japan Advanced Institute of Science and Technology for offering NMR experimental time and their useful discussions. We also thank Dr. Yoshihiro Mori of Faculty of Pharmaceutical Sciences, Toyama Medical and Pharmaceutical University for supporting CD experiments. This work was supported by Grants-in-Aid for Scientific Research (10308028) and the International Scientific Research Program (10044048) from the Ministry of Education, Science and Culture of Japan, and the Program for Promotion of Basic Research Activities for Innovative Bioscience (Japan).

References

[1] I. Laczko, M. Hollosi, E. Vass, Z. Hegedus, E. Monostori, G.K. Toth, Biochem. Biophys. Res. Commun. 242 (1998) 474–479.
[2] T. Raha, D. Chattopadhyay, D. Chattopadhyay, S. Roy, Biochemistry 38 (1999) 2110–2116.
[3] T. Raha, E. Samal, A. Majumdar, S. Basak, D. Chattopadhyay, D.J. Chattopadhyay, Protein Eng. 13 (2000) 437–444.
[4] S. Ohki, M. Eto, E. Kariya, T. Hayano, Y. Hayashi, M. Yazawa, D. Brautigan, M. Kainosho, J. Mol. Biol. 314 (2001) 839–849.
[5] E. Rabon, M.A. Reuben, Annu. Rev. Physiol. 52 (1990) 321–344.
[6] K. Togawa, T. Ishiguro, S. Kaya, A. Shimada, T. Imagawa, K. Taniguchi, J. Biol. Chem. 270 (1995) 15475–15478.
[7] K. Togawa, S. Kaya, A. Shimada, T. Imagawa, S. Mårdh, J. Corbin, U. Kikkawa, K. Taniguchi, Biochem. Biophys. Res. Commun. 227 (1996) 810–815.
[8] M. Kanagawa, S. Watanabe, S. Kaya, K. Togawa, T. Imagawa, A. Shimada, K. Kikuchi, K. Taniguchi, J. Biochem. 127 (2000) 821–828.
[9] M. Kanagawa, S. Kaya, H. Umezu, S. Watanabe, K. Togawa, A. Shimada, T. Imagawa, S. Mårdh, K. Taniguchi, J. Biochem. 126 (1999) 266–270.
[10] M.S. Feschenko, K.J. Sweadner, J. Biol. Chem. 272 (1997) 17726–17733.
[11] E. Féraille, M.L. Carranza, S. Gonin, P. Béguin, C. Pedemonte, M. Rousselot, J. Caverzasio, K. Geering, P.Y. Martin, H. Favré, Mol. Biol. Cell 10 (1999) 2847–2859.
[12] T. Toyofuku, K. Kurzydlowski, N. Narayanan, D.H. MacLennan, J. Biol. Chem. 269 (1994) 26492–26496.
[13] A.V. Chibalin, C.H. Pedemonte, A.I. Katz, E. Féraille, P.O. Berggren, A.M. Bertorello, J. Biol. Chem. 273 (1998) 8814–8819.
[14] A.V. Chibalin, G. Ogimoto, C.H. Pedemonte, T.A. Pressley, A.I. Katz, E. Féraille, P.O. Berggren, A.M. Bertorello, J. Biol. Chem. 274 (1999) 1920–1927.
[15] G.A. Yudowski, R. Efendiev, C.H. Pedemonte, A.I. Katz, P.O. Berggren, A.M. Bertorello, Proc. Natl. Acad. Sci. USA 97 (2000) 6556–6561.
[16] Y.H. Chen, J.T. Yang, H.M. Martinez, Biochemistry 11 (1972) 4120–4131.
[17] L. Braunschweiler, R.R. Ernst, J. Magn. Reson. 53 (1983) 521–528.

[18] A. Bax, D.G. Davis, J. Magn. Reson. 65 (1985) 355–360.
[19] J. Jeener, B.N. Meier, P. Bachmann, R.R. Ernst, J. Chem. Phys. 71 (1979) 4546–4553.
[20] F. Delaglio, S. Grzesiek, G. Vuister, G. Zhu, J. Pfeifer, A. Bax, J. Biomol. NMR 6 (1995) 277–293.
[21] C. Bartels, T.H. Xia, M. Billeter, P. Güntert, K. Wüthrich, J. Biomol. NMR 5 (1995) 1–10.
[22] A.T. Brünger, X-PLOR Manual, Version 3.1, Yale University, New Haven, CT, USA, 1993.
[23] R.A. Laskowski, M.W. MacArthur, D.S. Moss, J.M. Thornton, J. Appl. Crystallogr. 26 (1993) 283–290.
[24] R. Koradi, M. Billeter, K. Wüthrich, J. Mol. Graph. 14 (1996) 51–55.
[25] K. Wüthrich, NMR of Proteins and Nucleic Acids, Wiley, New York, 1986.
[26] C. Toyoshima, M. Nakasako, H. Nomura, H. Ogawa, Nature 405 (2000) 647–655.
[27] A.W. Jude, W. Anthony, A.M. David, J. Biol. Chem. 276 (2001) 43197–43204.
[28] F. Festy, J.-C. Robert, R. Brasseur, A. Thomas, J. Biol. Chem. 276 (2001) 7721–7726.
[29] F.D. Sönnichsen, J.E. Van Eyk, R.S. Hodges, B.D. Sykes, Biochemistry 31 (1992) 8790–8798.
[30] E. Féraille, M.L. Carranza, S. Gonin, P. Béguin, C. Pedemonte, M. Rousselot, J. Caverzasio, K. Geering, P.Y. Martin, H. Favré, Mol. Biol. Cell 10 (1999) 2847–2859.